Journal Name

ARTICLE TYPE

Cite this: DOI: 00.0000/xxxxxxxxxx

Supplementary information: Perspectives for CdSe/CdS Spherical Quantum Wells as Rapid-Response Nano-Scintillators

Zhu Meng,[a] Benoit Mahler,[a] Julien Houel,[a] Florian Kulzer,[a] Gilles Ledoux,[a] Andrey Vasil'ev[b], and Christophe Dujardin *[a]

1 Synthesis

1.1 Chemicals and materials

1-dodecanethiol (DDT, 98%), cadmium nitrate tetrahydrate (>99%), trioctylphosphine (TOP, 97%) and 1-octadecene (ODE, 90%) were purchased from Sigma Aldrich. cadmium oxide (CdO, 99.99%), selenium (99.9%), sulfur (99.99%) were purchased from Strem. Ethanol (>=99%) and hexane were purchased from Carlo Erba. Methanol (98.5%) and toluene (99.9%) were purchased from VWR. Oleic acid (OA, 90%), oleylamine (OAm, 80-90%) and sodium myristate (>98%) were purchased from Alfa-aesar, Acros and TCI respectively. All chemicals were used as received without any further purification.

1.2 Preparation of precursors

$Cd(myr)_2$. is prepared according to a procedure published previously[1]. 9.3 g sodium myristate was dissolved in 750 mL methanol and stirring until completely dissolved (1h). And 3.7 g cadmium nitrate dissolved in 120 mL methanol was mixed into the above solution and stirred slowly to obtain white precipitate(1 h). Then the precipitate was filtered by a Buchner funnel, rinsed several times with methanol and dried under vacuum overnight. 0.25M S-ODE. 20 mL ODE was degassed under vacuum for 30 min at 70 °C to evacuate oxygen and water (P<0.3 mbar), and the reaction was performed under argon gas condition and 160 mg sulfur powder was added into flask. Then the temperature was heated up to 140 °C until all the sulfur powder was dissolved, and the flask was kept at 80 °C to prevent sulfur powder from being precipitated out of solution. 0.5M $Cd(OA)_2$ in OA. 6.42 g CdO was dissolved in 100 mL oleic acid at 180 °C. when the mixture was slightly yellow and transparent, decrease the temperature to 120 °C to avoid the $Cd(OA)_2$ degrade at high temperature. Then degas the flask until P<0.3 mbar. 0.5M $Cd(OA)_2$ in OA/ODE. 6.42 g CdO was dissolved in 50 mL oleic acid and 50 mL ODE at 160 °C for 30 mins under argon, and degas at 100 °C for 90 mins. Comparing to the 0.5 M $Cd(OA)_2$ in OA, the existence of ODE can prevent the nanoparticles from degrading by oleic acid. 2M TOPSe. 1.58 g Se powder was added in 10 mL TOP at 100 °C for 4 h until dissolved completely. The reaction was performed in glove box to exclude the influence of oxygen. Then TOPSe was stocked under inert gas atmosphere.

1.3 Synthesis protocol

Spherical quantum wells synthesis is a three steps process[2]. CdS seeds are formed through homogeneous nucleation, and followed by a thin CdSe emissive layer synthesis. The subsequent shell growth is performed to cover different thickness shell on CdS/CdSe-based nanocrystals. For this subject, we are interested in samples coated by very thick shell, thus continuous injection of shell precursors was chosen to fulfill the formation of emissive layer and shell.

The specific experimental steps and parameters are as follows: Synthesis of CdS seeds. 1.5 mL 0.5 M $Cd(OA)_2$ in OA/ODE and 27 mL ODE were degassed under vacuum and argon for three times. Under flowing argon, the flask was heated up to 270 °C, and inject 1.5 mL S-ODE (0.25 M) at this temperature. Afterwards, decrease temperature to 250 °C immediately to undergo the growth process for 15 mins. After cooling down the mixture to room temperature, the samples were purified by precipitation with ethanol, centrifugated at high speed and redispersed in hexane. The CdS seeds are around 1.3 nm in diameter. Synthesis of CdSe layer. 2.7 mL CdS seeds at 193 μM and 5 mL ODE were degassed under vacuum at 65 °C for 1 h. The prepared 0.1M precursors mixtures (0.6 mL TOPSe, 2.4 mL $Cd(OA)_2$ in OA/ODE and 9 mL ODE) was injected at 6 mL/h at 300 °C. 11.2 mL mixture was consumed for the desired size emission layer. The solution is cooled down to room temperature, and the sample was precipitated with ethanol, toluene and OA. The final sample is suspended in hexane. The thickness of this layer is around 1.8 nm. Synthesis of CdS shell. 3 mL CdS/CdSe (52 μM), 85 mg $Cd(myr)_2$ and 10 mL ODE are introduced in a three-neck flask. $Cd(myr)_2$ is added to prevent the degradation of CdS/CdSe at high temperature. After 30 mins of degassing under vacuum at 65 °C, the solution was heated up to 305 °C and 1 mL OAm was injected to form

[a] Institut Lumière Matière, UMR5306 Université Lyon 1-CNRS, Université de Lyon, 69622 Villeurbanne cedex, France; E-mail: christophe.dujardin@univ-lyon1.fr
[b] Skobeltsyn Institute of Nuclear Physics, Lomonosov Moscow State University, 119991 Moscow, Russia.

† Electronic Supplementary Information (ESI) available: [details of any supplementary information available should be included here]. See DOI: 00.0000/00000000.

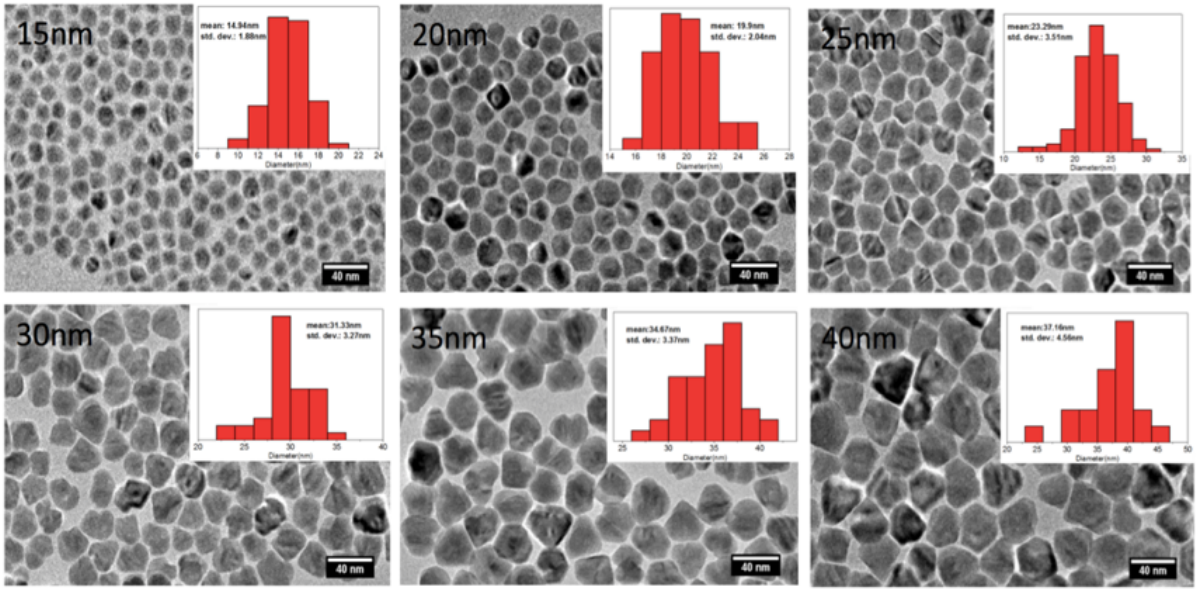

Fig. 1 Transmission electron microscopy image of SQWs with 15 nm-40 nm diameter, respectively, indicating the multi-faceted and irregular shapes. (inset: size distribution histogram with mean diameter and the standard deviation).

monodispersed nanoparticles. Cd and S precursors were prepared as 0.2M solution of 1.5 mL DDT diluted in 31.42 mL ODE, and of 13.2 mL $Cd(OA)_2$ in OA/ODE dissolved in 15.8 mL ODE and 4 mL OAm. The precursors are injected continuously into the flask by two syringes at 0.8 nm/h under argon. Taking aliquots from flask at desired size, 15 nm, 20 nm, 25 nm, 30 nm, 35 nm, 40 nm in diameter. The aliquots are reheated up directly to 305 °C, 1.5 mL $Cd(OA)_2$ in ODE is added to passivate the surface of SQWs. After 30 mins annealing, the reaction was cooled down to room temperature. The nanoparticles are precipitated and redispersed with ethanol and hexane. Then the samples are suspended in hexane. 35 nm and 40 nm samples are unable to suspend in hexane due to their large size. For characterization, toluene has a good performance to disperse these large sized samples at low concentration.

2 Characterizations

2.1 Structural and optical characterizations

The morphology of the SQWs was characterized with a transmission electron microscope (TEM, JEOL JEM 2010) operating at an accelerating voltage of 200 kV. Samples for TEM characterization were prepared by placing a drop of a dilute nanocrystal solution onto a carbon-coated copper grid, followed by degassing overnight. The SQWs are found to exhibit the multi-faceted and irregular shapes (Figure S1), which is often observed in large core/shell QDs[3]. The absorption measurements were realized on an AvaSpec-2048L versatile fiber-optic spectrometer, which is used for measurements in the UV-VIS-NIR spectral range (200 to 1100 nm). The photoluminescence spectra were acquired by an Edinburgh FS5 fluorescence spectrophotometer (Edinburgh Instruments Ltd, UK) with a Xenon lamp excitation at 350 nm. PL QY of film samples was measured by absolute method. The setup is equipped with an integrating sphere(Labsphere) and the spectrometer(AvaSpec-2048) and the excitation wavelength is 450 nm.

2.2 Time-resolved measurements

Pulsed X-rays with energies up to 30 keV were generated with a repetition rate of 500kHz by a picosecond diode laser at 405 nm (Delta diode from Horiba) focused on a X-ray tube (model N5084 from from hamamatsu). In the case of optical excitation, the same laser (405 nm) was focused on the sample using a X32 microscoscope objective. The resulting photons were collected by Kymera spectrograph (ANDOR) and detected by an hybrid PMT XXX. For decay-time measurements, the photons were histogramed using a PicoHarp300 time-correlated single-photon counting (64 ps time/bin) and for the time resolved spectra a MCS6A multiple-channel time analyser was used (800 ps time/bin). To prepare the sample, the SQWs was redispersed in a solution of hexane: octane (9:1). The mixture of hexane and octane can dry homogeneously avoiding the coffee-ring effect that concentrates the NCs on the border of the drop[3]. The films were obtained by dropcasting respectively 40 μL, 20 μL, 20 μL and 10 μL of solution concentrated at 3.5 μM, 0.87 μM, 0.57 μM and 0.77 μM and then the films were left to dry several minutes.

2.3 Lifetime measurements in confocal geometry

Optical, high excitation intensities, lifetime measurements were carried out on a home-build confocal microscope setup[4]. Optical excitation was provided by a filtered, pulsed supercontinuum source (SuperK Fianum NKT) centered at 420 nm with a 15 nm bandwidth. The PL signal from the SQWs thin-films was sent to a single photon avalanche diode (SPAD, ARQH-50 Perkin elmer), after a filtering stage operated by a long-pass 600 nm (FLEH0600) or a band-pass 650±20 nm (FBH0650-40). The instrument response function (IRF) of the system exhibits a 700 ps response.

In order to have a precise value of the exciton number per SQW per pulse $< N >$, the excitation spot size was determined to be $1.25\,\mu$m (see Figure S2). To minimize the potential damage to the SQWs at high excitation energy, the sample is scanned *via* the xy piezo during all measurements, at rate of $10\,\mu$m/s.

3 Simulation

The electronic excitations in NCs strongly interact with each other with different kinds of transformations like scattering with production of new electronic excitations, scattering with exchange of energy between excitations, Auger processes etc. During all these processes the total energy in electron subsystem of an excited NC is conserved. We have to take into account some non-conserving processes like phonon emission and electron escape from NP. In such approximations we can describe the electronic state of NP using the populations $n_{N_eN_h}(E,t)$ with certain total energy and certain numbers of excited electrons N_e and holes N_h. When we describe the initial stages of relaxation with total energy higher than the forbidden gap energy, we can neglect the Coulomb interaction energy (or distribute it over all excitations). The energy of this multi-excitation state can be written then as

$$E_{N_eN_h} = \sum_{p=1}^{N_e} E_{ep} + \sum_{q=1}^{N_h} E_{hq}. \tag{1}$$

The origin of the energies is taken at the top of the valence band of CdSe, and both electron and hole energies are positive (the more deeper hole, the higher its energy). The set of rate equations which describe the evolution of multi-excitation system can be written as

$$\begin{aligned}
&\frac{\partial n_{N_eN_h}(E,t)}{\partial t} - S_{N_eN_h}(E)\frac{\partial n_{N_eN_h}(E,t)}{\partial E} = \\
&- P_{N_eN_h}(E)\,n_{N_eN_h}(E,t) + P_{N_e-1,N_h-1}(E)\,n_{N_e-1,N_h-1}(E,t) \\
&- Q_{N_eN_h}(E)\,n_{N_eN_h}(E,t) + Q_{N_e+1,N_h+1}(E)\,n_{N_e+1,N_h+1}(E,t) \\
&- \frac{n_{N_eN_h}(E,t)}{\tau_{N_eN_h}(E)} + \frac{n_{N_e+1,N_h+1}(E+E_{ex},t)}{\tau_{N_e+1,N_h+1}(E+E_{ex})} \\
&- n_{N_eN_h}(E,t)\int K_{N_eN_h}(E,E')\,dE' + \\
&+ \int K_{N_e+1,N_h}(E',E)\,n_{N_e+1,N_h}(E',t)\,dE' \\
&- \left(\beta n_{N_eN_h}(E,t) - \beta n_{N_e-1,N_h}(E+W,t)\right)n_f(t).
\end{aligned} \tag{2}$$

Terms with S describes the rates of phonon emission, P - production of $e-h$ pairs, Q - Auger processes, τ describe radiation time, K electron escape, and β - electron capture from surrounding media.

Here E_{ex} is exciton energy, W is work function energy, n_f is the concentration of electrons in the surrounding media. Rate coefficients $S_{N_eN_h}$, $P_{N_eN_h}$, $Q_{N_eN_h}$, $\tau^{-1}_{N_eN_h}$ are proportional to the square of the process matrix element and the density of final states. The densities of final states plays the important role since they define the possibility of the processes due to energy conversation law. Let us discuss the formation of multi-excitation densities of states $\rho_{N_eN_h}(E)$. The density of one-particle states for electrons and holes are $\rho_{10}(E_e) = \rho_e(E_e)$ and $\rho_{01}(E_h) = \rho_h(E_h)$, correspondingly. Band structure calculations gives the value of density of states per unit cell per electron-volt $\rho^{\text{CdS, 1 unit cell}}_{e(h)}(e(h))$ and $\rho^{\text{CdSe, 1 unit cell}}_{e(h)}\left(E_{e(h)}\right)$. The number of unit cells equals to the volume of the compound over the volume of the unit cell v_{CdS} and v_{CdSe} for these compounds. Therefore one can easily estimate the number of unit cells $n_{\text{CdSe}} = 4\pi\left(r_w^3 - r_c^3\right)/3v_{\text{CdSe}}$ and $n_{\text{CdS}} = 4\pi\left(r_s^3 - r_w^3 + r_c^3\right)/3v_{\text{CdS}}$ (here r_w, r_c and r_s are radii of the well, core and shell, correspondingly). The overall density of states equals to

$$\begin{aligned}
\rho_{e(h)}\left(E_{e(h)}\right) =& n_{\text{CdSe}}\rho^{\text{CdSe, 1 unit cell}}_{e(h)}\left(E_{e(h)}\right) \\
&+ n_{\text{CdS}}\rho^{\text{CdS, 1 unit cell}}_{e(h)}\left(E_{e(h)}\right) \\
\equiv& \rho^{\text{CdSe}}_{e(h)}\left(E_{e(h)}\right) + \rho^{\text{CdS}}_{e(h)}\left(E_{e(h)}\right).
\end{aligned} \tag{3}$$

The density of states consisted of one electron and one hole can be estimated as

$$\rho_{11}(E) = \iint \rho_e(E_e)\,\rho_h(E_h)\,\delta(E - E_e - E_h)\,dE_e dE_h, \tag{4}$$

if we neglect Coulomb interaction of particles. In general case

$$\begin{aligned}
\rho_{N_eN_h}(E) =& \int\cdots\int \prod_{p=1}^{N_e}\rho_e(E_{ep}) \prod_{q=1}^{N_h}\rho_h(E_h) \\
&\times \delta\left(E - \sum_{p=1}^{N_e}E_{ep} - \sum_{q=1}^{N_h}E_{hq}\right)\prod_{p=1}^{N_e}dE_{ep}\prod_{q=1}^{N_h}dE_{hq}.
\end{aligned} \tag{5}$$

If we introduce Fourier transformation of the density of states,

$$\widetilde{\rho}_e(z) = \int_{-\infty}^{\infty}\rho_e(E)\,e^{izE}dE, \qquad \rho_e(E) = \frac{1}{2\pi}\int_{-\infty}^{\infty}\widetilde{\rho}_e(z)\,e^{-izE}dz, \tag{6}$$

and the analogous transformation for hole density of states, multiple integral in Eq. (5) can be calculated as

$$\rho_{N_eN_h}(E) = \frac{1}{2\pi}\int_{-\infty}^{\infty}\widetilde{\rho}_e(z)^{N_e}\,\widetilde{\rho}_h(z)^{N_h}\,e^{-izE}dz. \tag{7}$$

Using these notations, the rate coefficient for phonon relaxation can be written as

$$\begin{aligned}
S_{N_eN_h}(E) =& \frac{1}{2\pi\rho_{N_eN_h}(E)}\int_{-\infty}^{\infty}\Big(N_e\widetilde{s}_e(z)\,\widetilde{\rho}_e(z)^{N_e-1}\,\widetilde{\rho}_h(z)^{N_h} \\
&+ N_h\widetilde{s}_h(z)\,\widetilde{\rho}_e(z)^{N_e}\,\widetilde{\rho}_h(z)^{N_h-1}\Big)\,e^{-izE}dz,
\end{aligned} \tag{8}$$

where

$$\widetilde{s}_{e(h)}(z) = \int_{-\infty}^{\infty}s_{e(h)}(E)\,\rho_{e(h)}(E)\,e^{izE}dE, \tag{9}$$

and we take into account that each electron and hole can loose energy due to phonon emission with rates $s_e(E_e)$ and $s_h(E_h)$, cor-

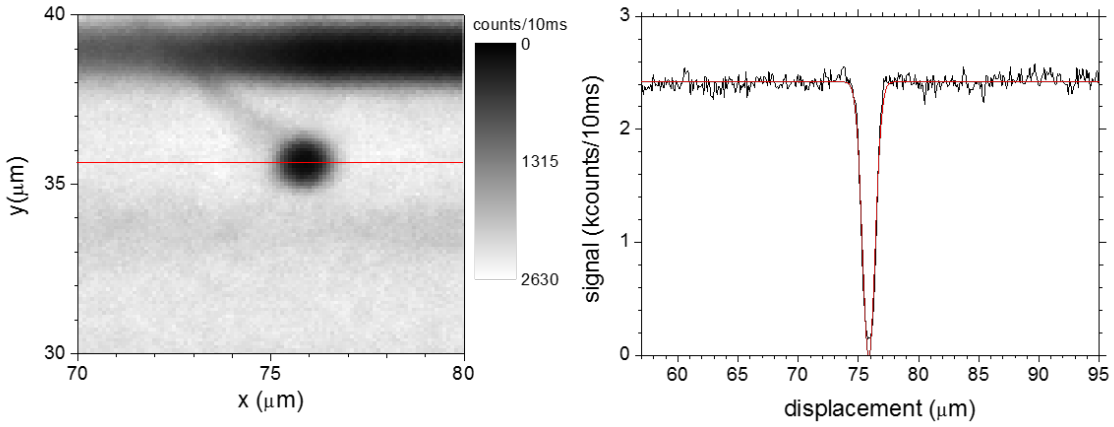

Fig. 2 left: image of the laser spot and right deduced profile fitted allowing to determined a spot diameter of 1.25 μm.

respondingly. For parabolic band with mass m_e the energy loss rate $s_e(E)$ due to emission and absorption of longitudinal optical phonons with energy $\hbar\Omega_{LO}$ equals to

$$s_{e(h)}(E) = 2\Omega_{LO}^2 \frac{Ry^* a_B^*}{\varepsilon^* \sqrt{2E/m_{e(h)}}} \ln\frac{4E}{\hbar\Omega_{LO}}. \tag{10}$$

Here Ry^* and a_B^* are effective Rydberg constant and Bohr radius, correspondingly, and ε^* is effective dielectric permittivity without account for electronic excitations.

Similarly, the rate of production of new electron-hole pair

$$P_{N_eN_h}(E) = \frac{1}{2\pi\rho_{N_eN_h}(E)} \int_{-\infty}^{\infty} \Big(N_e \widetilde{p}_e(z)\, \widetilde{\rho}_e(z)^{N_e-1}\, \widetilde{\rho}_h(z)^{N_h} + N_h \widetilde{p}_h(z)\, \widetilde{\rho}_e(z)^{N_e}\, \widetilde{\rho}_h(z)^{N_h-1} \Big) e^{-izE} dz, \tag{11}$$

where

$$\widetilde{p}_{e(h)}(z) = \int_{-\infty}^{\infty} p_{e(h)}(E)\, \rho_{e(h)}(E)\, e^{izE} dE, \tag{12}$$

and

$$p_{e(h)}(E) = \int_0^E \kappa_{e(h)}(E, E-\hbar\omega)\, \mathrm{Im}\left(-\frac{1}{\varepsilon(\hbar\omega)}\right) \times \rho_{e(h)}(E-\hbar\omega)\, \rho_{11}(\hbar\omega)\, d(\hbar\omega). \tag{13}$$

Here $\kappa_{e(h)}(E,E')$ is the mean value of the square of transition matrix element of an electron (hole) from state with energy E to E' with corresponding coefficients, which describes the process of inelastic scattering of an electron with production of a virtual longitudinal photon with energy $\hbar\omega = E - E'$. For simplicity we can neglect the energy dependence of two first factors in the integral in Eq. (13), and get the estimation which takes into account only densities of states and restrictions due to energy conservation laws: $p_{e(h)}(E) = w_p \rho_{21(12)}(E)$, w_p is the parameter which describes the rate of the scattering process.

The emission of photons is supposed to occur only from CdSe region after the relaxation of electrons and holes into the SNW. Therefore we can estimate the radiation rate as

$$\tau_{NeNh}^{-1}(E) = \frac{w_r N_e N_h}{2\pi\rho_{N_eN_h}(E)} \int_{-\infty}^{\infty} \widetilde{\rho}_e^{\mathrm{CdSe}}(z)\, \widetilde{\rho}_h^{\mathrm{CdSe}}(z) \times \widetilde{\rho}_e(z)^{N_e-1}\, \widetilde{\rho}_h(z)^{N_h-1}\, e^{-izE} dz. \tag{14}$$

The factors Ne and N_h have combinatoric nature and ensures that the radiation rate τ_{22}^{-1} for bi-excitons is about 4 times larger than that for excitons τ_{11}^{-1}, for trions τ_{21}^{-1} and τ_{12}^{-1} are about 2 times larger than τ_{11}^{-1}. Here w_r is the parameter which describes the rate of the radiation process. For $N_e = 1$, $N_h = 1$ and $E < E_g^{\mathrm{CdS}}$ it is easy to demonstrate that $\tau_{11}^{-1} = w_r$.

The rate of Auger process $Q_{N_eN_h}(E)$ can be estimated as the rate of the reverse process of scattering with production of new $e-h$ pair, assuming (as for the radiation processes) that the interaction of $2e+h$ or $e+2h$ occurs mainly if these particles are located in SNW:

$$Q_{N_eN_h}(E) = \frac{w_q}{2\pi\rho_{N_eN_h}(E)} \int_{-\infty}^{\infty} \Big(N_e(N_e-1) N_h \widetilde{\rho}_e^{\mathrm{CdSe}}(z)^2\, \widetilde{\rho}_h^{\mathrm{CdSe}}(z) \times \widetilde{\rho}_e(z)^{N_e-2}\, \widetilde{\rho}_h(z)^{N_h-1} + N_e N_h (N_h-1)\, \widetilde{\rho}_e^{\mathrm{CdSe}}(z)\, \widetilde{\rho}_h^{\mathrm{CdSe}}(z)^2 \times \widetilde{\rho}_e(z)^{N_e-1}\, \widetilde{\rho}_h(z)^{N_h-2} \Big) e^{-izE} dz. \tag{15}$$

The rate of electron escape from the nanoparticle can be estimated as

$$K_{N_eN_h}(E,E') = N_e \frac{\rho_{N_e-1,N_h}(E')}{\rho_{N_eN_h}(E)} k_e(E-E')\, \rho_e(E-E') \tag{16}$$

using the solution of diffusion problem for escape of electron with energy above the work function energy W from the sphere with

shell radius r_s:

$$k_e(E) = \frac{3}{r_s}\sqrt{\frac{2E}{m_e}}\begin{cases} 0, & E < W; \\ \frac{(E-W)\left(W^2+EW+2E^{3/2}\sqrt{E-W}-2E^2\right)}{EW^2}, & E \geq W. \end{cases} \quad (17)$$

Here we do not consider the terms with electrons returning to the nanoparticle from the surrounding media.

For the solution of rate equation (2) one need the estimation of initial energy distribution of the excitations in nanoparticle. We suppose that fast electron loss the energy proportional to $\mathrm{Im}\left(-\frac{1}{\varepsilon(\hbar\omega)}\right)$, where one can average the dielectric permittivity according to the weight fractions of CdS and CdSe. In reality we need to correct this distribution with account for surface plasmon resonances in spherical nanoparticle, so the energy distribution should take into account some terms with account some Mie effects like $\mathrm{Im}\left(-\frac{1}{\varepsilon(\hbar\omega)+f_n}\right)$, $1 \leq f_n < 2$. In this case the peak of energy distribution is shifted to lower energies in comparison with bulk plasmon energy. In the initial state each scattering of fast ionizing electron produces one electron-hole pair. There can be multiple scatterings in nanoparticles with rather big shell radius. Therefore ionizing electron can initially create few hot electron-hole pairs.

Notes and references

1 Y. A. Yang, H. Wu, K. R. Williams and Y. C. Cao, *Angew. Chem. Int. Ed.*, 2005, **44**, 6712–6715.

2 B. G. Jeong, Y.-S. Park, J. H. Chang, I. Cho, J. K. Kim, H. Kim, K. Char, J. Cho, V. I. Klimov, P. Park *et al.*, *ACS nano*, 2016, **10**, 9297–9305.

3 M. Nasilowski, P. Spinicelli, G. Patriarche and B. Dubertret, *Nano lett.*, 2015, **15**, 3953–3958.

4 A. Aubret, J. Houel, A. Pereira, J. Baronnier, E. Lhuillier, B. Dubertret, C. Dujardin, F. Kulzer and A. Pillonnet, *ACS Appl. Mater. Interfaces*, 2016, **8**, 22361–22368.